ELSEVIER

Journal of Arid Environments 69 (2007) 237–258

Journal of Arid Environments

www.elsevier.com/locate/jaridenv

Seasonal water dynamics of a sky island subalpine forest in semi-arid southwestern United States

C. Brown-Mitic[a,*], W.J. Shuttleworth[b], R. Chawn Harlow[c], J. Petti[b], E. Burke[c], R. Bales[d]

[a]*Atmospheric Science Program, Geography Department, Indiana University, 701 E. Kirkwood Ave., Bloomington, Indiana 47405, USA*

[b]*SAHRA, University of Arizona, Tucson, AZ, USA*

[c]*Met Office, Devon, UK*

[d]*University of California, Merced, CA. USA*

Received 12 January 2006; received in revised form 9 September 2006; accepted 11 September 2006
Available online 27 November 2006

Abstract

This paper describes the first results from a hydro-micrometeorological study designed to characterize the surface exchanges of water, and CO_2, at a sky island forest site in the Santa Catalina Mountains. Data collected between June 2002 and December 2004 is used to describe the seasonal water/carbon dynamics of this ecosystem. During the severely dry pre-monsoon period (May–June) when vapor pressure deficit exceeded 2 kPa, daytime relative humidity was below 20%, and soil moisture was less than 10%, the predominantly Douglas Fir/Pine forest severely reduced or curtailed its photosynthetic activity. At the onset of the monsoon season in July, the vegetation responded rapidly to the precipitation input, as soil moisture increased. The trees then remained relatively active throughout the fall and winter, particularly if there was adequate winter precipitation which promoted very high productivity into early spring. Given the relative importance of mountain island forest in this semi-arid landscape in terms of its contribution to area-average surface water and carbon exchange, the strong and somewhat unusual coupled seasonal cycles, this forest ecosystem likely has hitherto unrecognized implication for the seasonality of the regional-scale water and carbon cycle.

Keywords: Soil moisture; Latent heat flux; Evapotranspiration; CO_2 flux; Precipitation; Ecosystem exchange

*Corresponding author. Tel.: +1 812 856 5047; fax: +1 812 855 1661.
E-mail address: combrown@indiana.edu (C. Brown-Mitic).

0140-1963/$ - see front matter © 2006 Elsevier Ltd. All rights reserved.
doi:10.1016/j.jaridenv.2006.09.005

1. Introduction

The importance of understanding the surface atmosphere interactions of ecosystems, particularly the surface water and carbon fluxes is well established (Mitic et al., 1995; Baldocchi and Vogel, 1996; Baldocchi et al., 1997; Law et al., 2002). Knowledge of land surface exchange processes is integral to the understanding of phenomena such as the environmental water balance (Rouse, 2000) snowmelt dynamics (Neumann and Marsh, 1998; Nakai et al., 1999; Brown-Mitic et al., 2001), water resource predictions (Farah and Bastiaanssen, 2001; Carey and Woo, 2001), parameterizing global change models (Koster and Suarez, 1992), carbon sequestration (Monson et al., 2002; Gilmanov et al., 2003) and in general, the hydrological and carbon cycles (Shuttleworth, 1991; Mackay et al., 1998). Lessons learned from measuring and modeling surface exchanges have revealed the complexities that characterize surface–atmosphere exchange processes in ecosystems with complex micrometeorological dynamics (Rouse, 2000; Scott et al., 2000; Eugster et al., 2000) and in particular, forested ecosystems (Ogunjemiyo et al., 1997; Pattey et al., 1997; Baldocchi et al., 2000; Mahrt et al., 2000; Carrara et al., 2003) growing in complex terrain (Lee and Hu, 2002; Turnipseed et al., 2002). Semi-arid Sky Island Forest, a subset of the US western sub-alpine forest is an example of a forest ecosystem with such micrometeorological complexities. This forest ecosystem also experiences, on an annual basis, hydro-meteorological conditions which are becoming increasingly more frequent in the more expansive sub-alpine forests to the north and northeast of the region, which are significant sources of the regions' water resource. This research seeks to characterize the hydro-micrometeorology of a sky island sub-alpine forest, with its intermittent winter snow pack, and the explicit relationship between water availability and photosynthetic activities of the vegetation. This paper is the first step in that process and illustrates the seasonal characteristics of the forest vegetation–water relationship as observed during a 3-year period during which there were extreme drought conditions in the semi-arid southwestern United States.

Among the ecosystems present in the semi-arid environment of the Southwestern US, Sky Island Forest is unique and it has a unique relationship to the sparse surface-water resources available in the region. This ecosystem exists only at the top of mountains because it is only here that, as a long-term average, precipitation input exceeds evapotranspiration to the extent that forest vegetation can survive. Sky Island Forests, therefore, command potentially significant source areas for the water, some originally falling as snow, which ultimately leaves high ground to recharge aquifers in the plains below by way of mountain-front recharge. Quantifying and understanding the water, and related carbon cycling and budgets of this ecosystem is therefore of direct relevance to future projections of the sustainability of the water resources of US southwest.

Sky Island Forest grows on mountains that are isolated within the surrounding desert. The paucity of micrometeorological observations for this ecosystem is a result of the complexity of the terrain, the heterogeneity of the vegetation, the remoteness and inaccessibility of suitable study sites, and the availability of appropriate measurement techniques. The eddy covariance technique, which has proven effective for forest canopies (Pattey et al., 1997; Baldocchi et al., 1997; Geissbuhler and Siegwolf, 2000; Aubinet et al., 2000), was formerly thought to be unusable over sloping terrain prone to topographically modified flows and upslope/downslope advection, the latter being difficulty to measure or estimate. However, the overwhelming need to make observations in such environments has stimulated pioneering studies, which suggest that the use of the ec method may also be

appropriate for forested ecosystems with complex terrain (Al-Jiboori et al., 2000; Lee and Hu, 2002; Turnipseed et al., 2002). This paper relies heavily on the observations obtained at, and in the vicinity of an eddy covariance (ec) flux tower that is located in complex terrain on a sky island sub-alpine forest.

2. Site description

The field site is located (32° 25′ 00″ N, 110° 43′ 31″ W) in a second-growth subalpine mixed forest predominantly of Douglas Fir (*Pseudotsuga menziesii*) and Ponderosa Pine (*Pinus ponderosa*), on Mt. Bigelow, in the Santa Catalina Mountains of the Coronado National Forest northeast of Tucson, Arizona. The area has a basin and range topography with an average canopy height of 10 m, varying locally in the range of 4–19 m. Tree diameters are on average about 0.6 m and in the range of 0.3–2.2 m and the average Leaf Area Index (LAI) obtained from MODIS is approximately four.

The location of the flux tower and three micrometeorological stations is shown in Fig. 1a. The site is 2573 m above sea level and is located on a small plateau within a saddle area. The saddle has a generalized slope to the northwest of ~11%. The terrain within 1 km of the tower has a downward slope of ~17% to the south and ~11% to the west. There is at least 1 km of mature forest in most directions, and the southwestern edge of the saddle is more than 1 km from the tower. In the spring of 2002, an area of the forest beyond the northeastern edge of the saddle was burnt (Bullock fire). In June of 2003 the Aspen fire burnt a large portion of the forest (with controlled below canopy burns approximately 200 m from the tower). The forest canopy within at least 1 km of the tower site however was not burnt. The soil at the site is gravelly and cobbly with many stones, has a moderately coarse texture with an organic layer of a few centimeters and ~0.5 cm of litter. Soil depth is typically 0.25–1 m. There is no understory vegetation and no significant bodies of water in the vicinity of the site.

Air temperature rarely exceeds 32 °C in the summer or falls below −5 °C in the winter. The region is extremely dry, with daytime relative humidity below 30% for most of the year, except during the summer North American Monsoon season (Gochis et al., 2006), usually in July and August. The average annual total precipitation is 69–94 cm. Approximately 25% of the precipitation usually falls during the summer monsoon, the remainder been winter precipitation, which usually falls between December and March, a portion of which is in the form of snow. The relatively thin soil and steep slopes promote rapid surface runoff of summer rains. It is therefore the slow infiltration of winter precipitation that is most advantageous to ecosystem productivity. There is a strong inter annual variability in precipitation, with higher precipitation in El Niño winters and lower precipitation in La Niña winters. The year prior to the start of this study and during the study period, the surrounding region was in a state of drought with 2001 and 2002 receiving 69% and 64% of normal monsoon precipitation amounts (National Weather Service Forecast Office).

3. Material and methods

3.1. Instrumentation

In June of 2001 a network of four 3 m micrometeorological stations were installed in the vicinity of the planned site for a tall above canopy ec tower ~29 m (96 ft) in height.

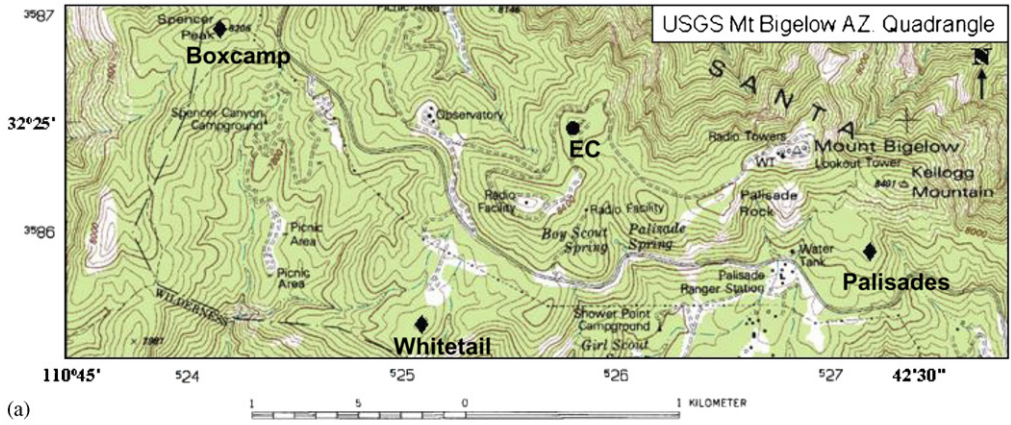

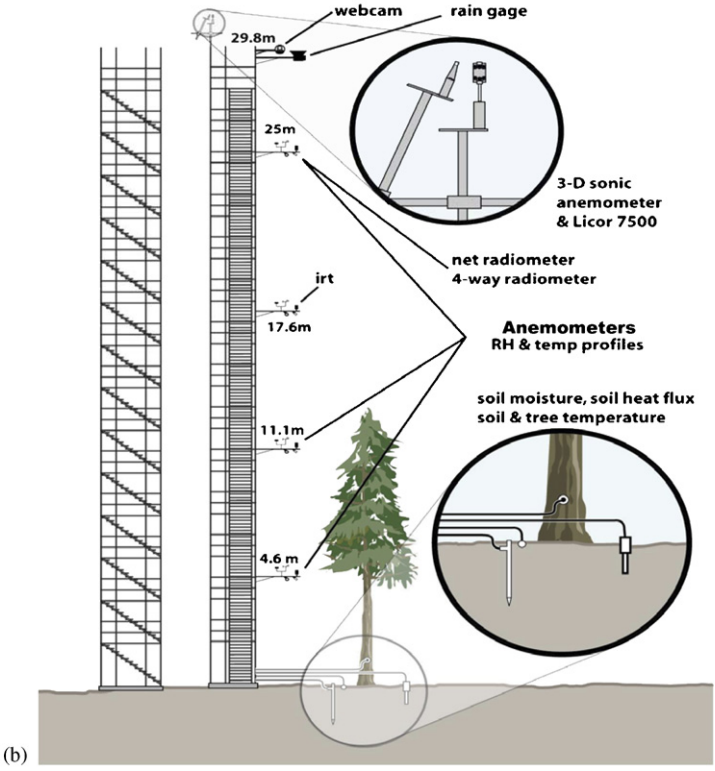

Fig. 1. (a) Topographic map of the Mt. Bigelow study site, showing the location of the eddy correlation tower (EC ♦) and the supporting micrometeorological stations of Boxcamp, Whitetail and Palisades (●), (b) Schematic diagram of the Mt. Bigelow eddy covariance flux tower instrumentation.

One station was located at the planned ec tower site, and the remaining three between 1 and 1.5 km southeast, southwest and northwest of the tower site (Fig. 1a.). These stations were equipped with wind, air temperature, relative humidity, surface and soil temperature, net radiation, precipitation and soil moisture sensors. The data from these stations was

used to characterize the variability in both the atmospheric and surface characteristics. The variability in surface temperature could be attributed to aspect and below canopy radiation conditions. However, atmospheric conditions were fairly consistent across all sites. In May of 2002 the ec tower was installed and instrumented. A schematic diagram of the ec tower instrumentation is given in Fig. 1b. Fluxes of water vapor, carbon dioxide and sensible heat were measured using an ec system. The ec system was mounted vertically at a height of 29.8 m on the NW corner the tower. Wind velocity and virtual temperature were measured with a three-dimensional ultra sonic anemometer (Gill WindMaster Pro) and CO_2 and water vapor were measured with an open-path infrared gas analyzer IRGA (Li-Cor 7500), the latter being mounted at an angle ($\sim 20^\circ$) with respect to the anemometer. Incoming and outgoing radiation components were measured above the canopy by a four-way radiometer (CNR-1 Kipp & Zonen) and net radiation by net radiometers (NR Lite Kipp & Zonen). Both of these radiometers were mounted at 25 m on the southern side of the tower. Rainfall was measured by a rain gauge mounted at the top of the tower ($\sim$29 m). An outdoor web camera was also mounted at the top of the tower. This camera could be controlled remotely from the University of Arizona but was otherwise automated to provide periodic vertical and horizontal panoramic views of the tower and surrounding areas, updated every 5 minutes at the project website and periodically archived.

The ec tower was also instrumented to measure micrometeorological data at three vertical levels. Wind (RM Young and later Visala 2D sonic), temperature and relative humidity sensors (Visala HMP45C) were mounted at 25 m to sample above-canopy conditions, at 11.1 m to sample within-canopy conditions, and 4.6 m, to sample below-canopy conditions. A net radiometer (Kipp & Zonen NR Lite) and an infrared thermometer (Apogee Precision), to measure the skin temperature of the ground, were mounted at a height of 4.6 m, while a second infrared thermometer mounted at 17.6 m measured canopy skin temperature.

Soil temperature was measured with three sets of multilevel thermocouple probes located at the surface, 2, 4, 8, 16, 32 and 64 cm, and soil heat flux was measured using three soil heat flux plates (REBS, HFT3-L) buried 2 cm deep in close proximity to the soil temperature probes. Soil moisture measurements were made with three sets of water content reflectometers (CS615) located in the vicinity of the soil temperature arrays and buried at depths of 6, 12, and 24 cm. Multiple sets of thermocouple temperature probes were installed at breast height in six nearby tree boles, integrating into the heartwood and across the xylem. These measurements were however problematic and the data considered unusable.

Periodic surveys of soil moisture were carried out using a portable soil moisture probe (CS620), at the ec tower and the meteorological stations. Soil survey markers were placed 10 meters apart for a distance of 100 m radiating out from the tower/station to the north, south, east and west. A survey transect was also established between the ec tower and the northwest station (Boxcamp). Soil/snow survey markers were places 100 m apart for a total of 16 survey points. The soil moisture surveys measured the integrated volumetric soil moisture in the top 10 cm of the soil. Snow surveys were also done during periods when there was snow accumulation.

Data from the ec system was sampled at 10 Hz, and 5-min average values were recorded for all other hydro-micrometeorological variables. Data acquisition from the ec system was made using a computer (PC) with a Linux operating system. The remaining sensors were monitored by data loggers which were periodically interrogated by the PC system, and the

data subsequently transferred to the computer hard drive. Data from the computer were downloaded and data exerts examined daily at the University of Arizona, via a high-speed data transmission line. Operations on the tower were powered by solar panels.

3.2. Data analysis

The surface fluxes were sampled and calculated using the ec technique, where flux contributions result from the covariance of the deviations of vertical wind (w') and a heat or scalar component (c') from their average, the mean wind velocities having first been rotated into a stream wise coordinate system (Kaimal and Finnigan, 1994). In the absence of direct measurement of vertical or horizontal advection such as described in Baldocchi et al. (2000), Lee and Hu (2002), Aubinet et al. (2003), estimations such as presented by Lee (1998) and Finnigan (1999), or the generation of a flow model for this site, is beyond the scope of this paper. This study focuses on the temporal patterns of exchange as opposed to mass budgets/balances. Possible advective contributions to the flux are neglected and it is assumed that there are no contributions from the residual Reynolds averaging terms. The total flux, F_c, of the variable c is therefore given by

$$F_c = \overline{\langle w\rangle\langle c\rangle} + \overline{\langle w^* c^*\rangle} + \overline{\langle w'c'\rangle} \tag{1}$$

where $w' = w - \bar{w}$, $c' = c - \bar{c}$, $\overline{\langle w\rangle\langle c\rangle}$ is the domain average flux, $\overline{\langle w^* c^*\rangle}$ is a possible low-frequency contribution to the flux, and $\overline{\langle w'c'\rangle}$ is the instantaneous flux. In general, the majority of the flux is usually in the $\overline{\langle w'c'\rangle}$ term and will be the flux term used in this study. Water vapour flux or evapotranspiration (ET), expressed as latent heat flux (LE), sensible heat flux (H), and carbon dioxide fluxes (CO_2) are gives as

$$\begin{aligned} \mathrm{LE} &= \lambda\overline{\langle w'q'\rangle} \\ H &= \overline{\langle w't'\rangle} \\ \mathrm{CO_2} &= \overline{\langle w'c'\rangle} \end{aligned} \tag{2}$$

where λ is latent heat of vaporization, q is water vapor concentration, t is sonic temperature, and c is CO_2 concentration. The EdiRe flux analysis software (John Moncrieff, School of Geosciences, University of Edinburgh) was used to calculate the fluxes. A uniform 30 min averaging window was adopted, and the Webb density correction (Webb et al., 1980) was applied to both the latent heat and CO_2 fluxes.

Given the location of the tower, in an area with relatively large changes in terrain' and the proximity of the recent forest fires, it is especially important to evaluate the source area of the observations. The flux footprint for the tower was calculated by a one-dimensional footprint model (Kaharabata et al., 1999), a formulation based on the concepts summarized by Horst and Weil (1992, 1994) that uses the shape component of Horst (1999). The results of these calculations are given in the next section.

Sample spectral analyses were made of the ec data, to investigate the possible extent of high-frequency flux loss due to averaging and/or sensor separation (Leuning and Judd, 1996; Massman, 2000). The average spectra over the ten 30-min periods between 08:00–13:00 local time on June 23, 2002, represents a typical summer day (Fig. A1). The power spectra of the sonic anemometer temperature, T', water vapor, q', and carbon dioxide, c', are all well behaved and exhibit an inertial subrange in the frequency range between 0.05 and 2–5 Hz. For the purposes of this study no correction was made for high

frequency loss. The $\langle w'T' \rangle$, $\langle w'c' \rangle$, and $\langle w'q' \rangle$ co-spectra show several peaks, some at the same frequency, suggesting there may be preferred length scales at which flux is transported above the forest.

Previous studies (e.g., Turnipseed et al., 2002; Wilson et al., 2002; Lee and Hu, 2002) have shown that achieving an energy balance between outgoing energy fluxes measured with the ec technique and the incoming radiant energy is problematic at sites with complex vegetation pattern, slope, and terrain. The nature of the study site is such that a comprehensive analysis of the energy budget is required, and will be presented in future publications. To indicate the general nature and magnitude of the issues involved in achieving energy closure at this site, the average measured turbulent and radiation fluxes for two sample periods (January 23–31, 2003 and May 22–31 2003) for which continuous data were available was calculated (Fig. A2). During the winter period, the mean closure was 101%, with a corresponding daytime closure of 101%. During the pre-monsoon period in May, the mean closure was 89% with a mean daytime closure of 74%. The better closure (~100%) during the winter may partially be explained by greater heat storage during the hot pre-monsoon/summer periods. The frequent clear sky conditions (and consequent strong stable atmospheric inversions) at night in this semi-arid environment result in significant under measurement of the outgoing nighttime energy fluxes.

3.3. Data quality control

To ensure good quality observations, extensive preliminary examination of the data was made. Hourly and daily time series were inspected to detect consistent anomalies and to ascertain that the measured variables were within a physically meaningful threshold and exhibited appropriate diurnal variations. Additionally, a 10 min averaging window was used to eliminate raw data values greater than ten times the standard deviation. The LICOR open path IRGA is particularly sensitive to the effect of surface moisture on the sensor, therefore the relevant diagnostic signals were checked and periods with moisture buildup removed. The mean and variance of all the calculated 30 min estimates were also checked for realism and to eliminate clearly anomalous data (often revealed as "spikes"). Based on observations made by Turnipseed et al. (2002) on variability in energy budget closure during upslope/downslope flows; visual inspection of the summer 2002–spring 2003 data (after initial filtering for bad data and anomalous spikes in the original raw 10 Hz data); the lower closure of the nighttime energy budget; the large uncertainty in the accurate sampling and interpretation of the nighttime flow regime in this terrain; and the observation that u^* below 0.15 typically occurs around 4 am when the footprint extends beyond 2 km, the decision was made to remove 30 min estimates with values greater than six standard deviation. This served to remove the residual unrealistic and questionable values from the calculated fluxes.

4. Results

4.1. Seasonal cycles

The weekly average air temperature for the period 1965–1980, ranges between 0 and 10 °C. Air temperature rarely drops below −7 °C or exceeds 27 °C, and surface/soil temperatures are typically at or above −1 °C. The long-term (1965–1980) average monthly

precipitation and the 2002–2004 monthly precipitation measured at or in the vicinity of the tower are shown in Fig. 2a. The distinct bimodal precipitation pattern is evident for the summer monsoon rainfall, and the winter precipitation. The pre-monsoon dry period is also a distinguishing feature particularly evident in the 2002–2004 precipitation amounts. It is also evident that the summer monsoon precipitation amounts are much less variable than the winter precipitation. Very large variability exists in the winter precipitation, which significantly affects the photosynthetic activity of the trees during the dry pre-monsoon period. During the period of this study the region had been in a state of extreme drought. During 2002, the monsoon precipitation was slightly above average, but there was no significant winter precipitation. The year 2003 had significantly higher than normal winter precipitation, and 2004 had lower than normal precipitation for both the winter and summer monsoon. All 3 years however had no significant precipitation during the three months (April, May, June) prior to the onset of the monsoon season. Fig. 2b shows soil moisture in the form of volumetric water content (vwc) measured at three depths (6, 12, and 24 cm). The annual bimodal pattern of winter precipitation and summer monsoon rainfall is strongly reflected in near-surface soil moisture as well as the vapor pressure deficit of the atmosphere. Prior to the monsoon season, in May and June of 2002, the air was very dry with vapor pressure deficit typically greater than 1.5 kPa at night, increasing to 2 kPa during the day. At this time, relative humidity was $\sim 20 \pm 10\%$. The soil had dried out after the winter rains and was very dry at ~10–15% vwc at all levels (Fig. 2b).

With the start of the monsoon rains, around day of year (DOY) 190, vapor pressure deficit fell to around 0.5 kPa, with relative humidity in the range 40–100%, depending on the time of day and whether there had been recent rain. Soil moisture increased quickly in response to the summer rainfall, especially near the surface, where it approached 40% for short periods (Fig. 2b). After the summer monsoon, the vapor pressure deficit rose to ~1.5 kPa during September (~DOY 270), and then fluctuated around 1 kPa during the winter season. The soil moisture again decreased to about 20% between the summer monsoon in 2002 and prior to the arrival of winter precipitation (Fig. 2b).

The variability in soil moisture at three of the micrometeorological stations is shown in Fig. 2c. There was a steady decrease in soil moisture from March to June at all three sites, with the Boxcamp site having slightly higher moisture content. The standard deviation for soil moisture observations across all sites ranged from 1.9 in March to 0.6 in June. The post-winter/pre-monsoon dry-down of the soil is a consistent feature, and is representative of the forest ecosystem soil moisture condition. Snow and soil moisture surveys were carried out from March to May of 2003, along a survey transect from the ec tower northwest to the Boxcamp station. There was consistent below canopy snow cover for the greater portion of March with a coefficient of variability of 10% at the beginning of March and 47% on March 20th. The greater and more persistent snow cover, towards the end of March, is at the Boxcamp end of the transect and accounts for the marginally higher soil moisture at that station. The coefficient of variability of soil moisture along the transect, ranged from 26% in March to 27% in May.

4.2. Source footprint and wind direction

The source area for the measured ec fluxes varies with the aerodynamic roughness of the underlying vegetation cover, the height of the sensors above the vegetation canopy, and the stability of the atmosphere. Calculations of the source footprint for the ec fluxes were made

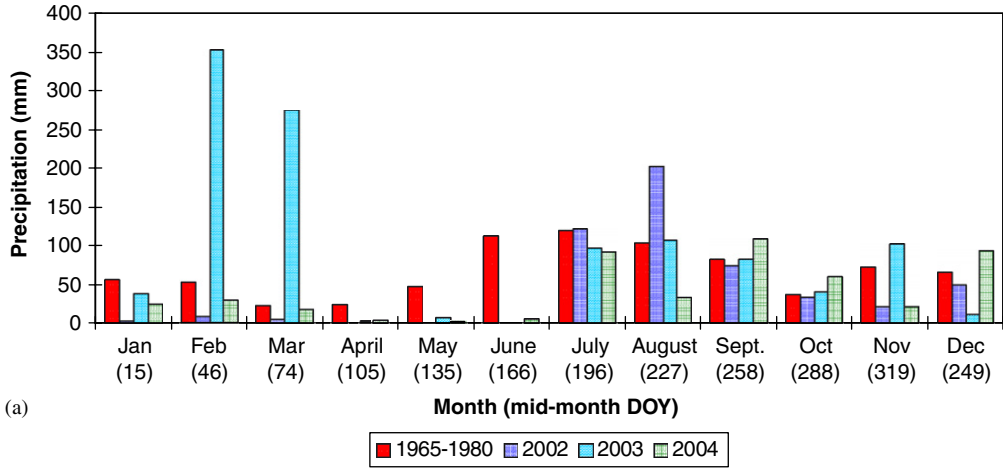

(a)

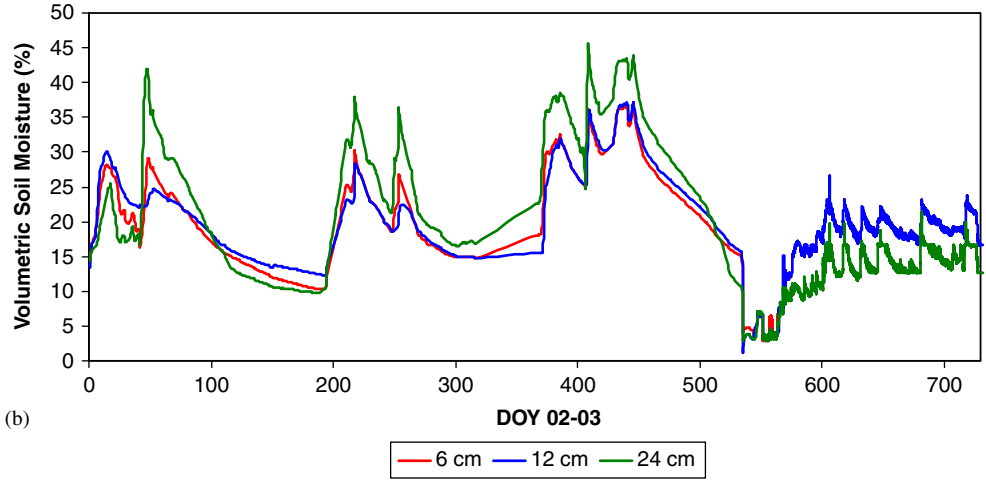

(b)

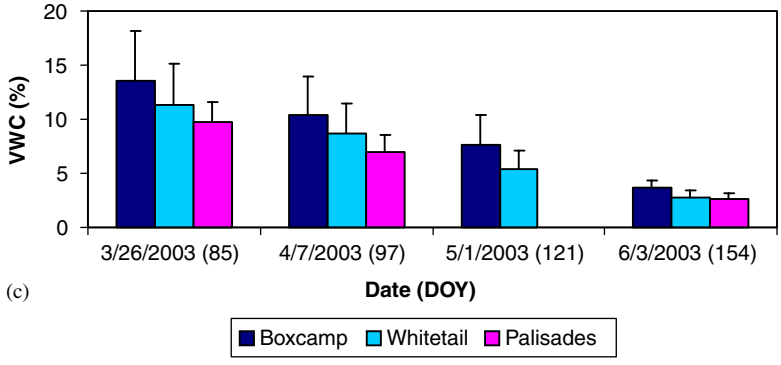

(c)

Fig. 2. (a) Monthly precipitation totals (mm) measured at and in the vicinity of the Mt. Bigelow tower. (b) Volumetric soil moisture measured at 6, 12 and 24 cm depths for 2002–2003, observed at Boxcamp micrometeorological station located in the vicinity of the Mt. Bigelow ec tower. (c) Average volumetric soil moisture at 5 cm depth observed during soil moisture survey conducted during the months of March to June of 2003 at the three meteorological stations within the vicinity of the Mt. Bigelow tower, depicted on Fig. 1a.

for an average forest canopy height of 10 m and an aerodynamic roughness of 2 m. The aerodynamic roughness value was selected based on a combination of the forest canopy characteristics and the complex nature of the terrain (Arya, 1988). The fractional contribution to the measured surface flux as a function of horizontal distance from the sensor for near neutral conditions ($z/L = 0.04$), highly unstable daytime conditions ($z/L = 1.9$) and stable nighttime conditions ($z/L = 0.7$) observed from June 2002 to January 2003 was calculated (Fig. A3). Under neutral conditions, 80% of the measured flux is estimated to have originated within 701 m. Under highly unstable situation, 80% of the flux source area is within 62 m of the tower, and under stable conditions 80% of the flux originated from within 2487 m of the tower. These values are of particular importance for the validity of the flux estimates given the complex nature of the terrain.

The dominant wind directions observed during 2003 and 2004 are illustrated in Fig. 3. Distinct seasonality was observed in the dominant wind direction. During the winter months (January to March), wind directions in the NW to SW quadrant had a frequency of 60%, during the pre-monsoon months of April to June, wind directions from N to NE had a frequency of 95%, and during the post-monsoon period, wind directions from the SW to SE quadrant had a frequency of 58%. During the monsoon season (July and August) there were two dominant wind directions. Wind directions from the NW to SW

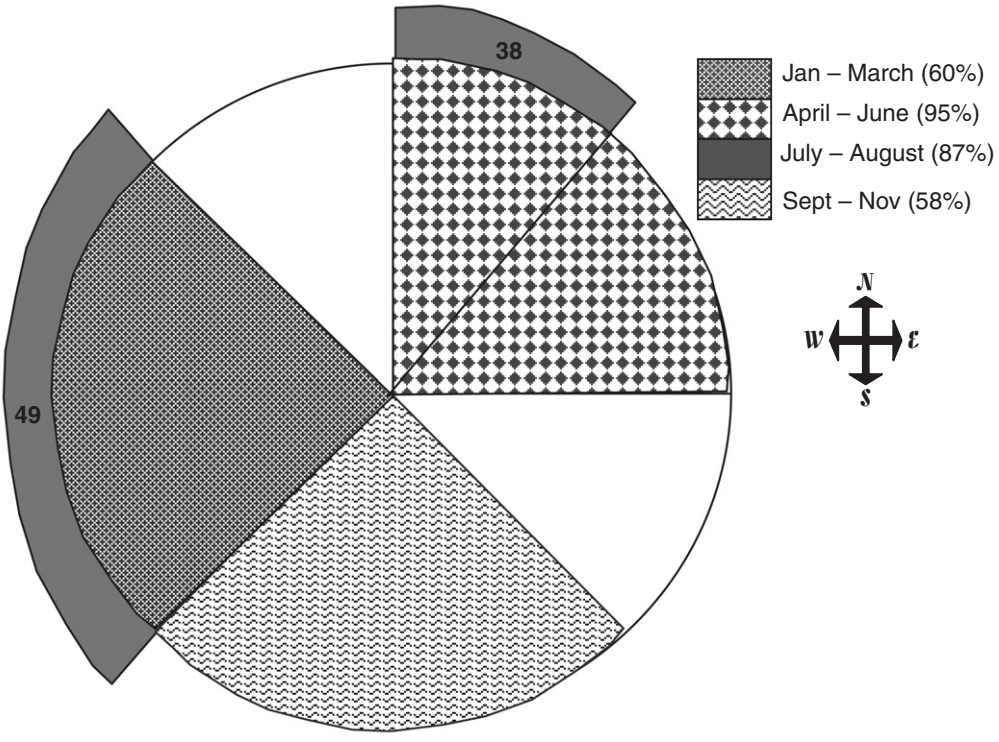

Fig. 3. Dominant wind direction, measured at the Mt. Bigelow ec tower, for seasonally distinct periods. January to March (winter), April to June (pre-monsoon), July to August (monsoon) and September to November (post-monsoon). The percentages are the frequencies of the associated wind direction.

quadrant had a frequency of 49% and N to NE winds had a frequency of 38%. The distribution of the dominant wind direction is important when considering the source area for the ec fluxes. In reference to Fig. 1a, the best forest canopy and fetch directions are $S \rightarrow E \rightarrow N$ of the ec tower. For the better part of the year the dominant wind directions were from these areas. It is however during the pre-monsoon drought season that the wind direction was from the least desirably direction, in terms of the fetch and forest canopy. Considering however, the footprint (62 m) during highly unstable conditions, the fluxes during this period may still be interpreted as originating from an area with suitable forest canopy cover.

4.3. Water and carbon fluxes

The seasonal trends for the exchange of water between the surface and the atmosphere, in the form of latent heat (evapotranspiration), sensible heat and CO_2 fluxes for the years 2003 and 2004 are shown in Fig. 4. There are two distinct drivers for the surface–atmosphere component of the carbon and water cycles for this ecosystem. While the turbulent energy fluxes of sensible and latent heat clearly reflects the seasonal trends in temperature, the CO_2 uptake by the trees was highest during the winter and prior to the pre-monsoon dry period. The magnitude of CO_2 uptake and assimilation by the trees corresponds to the amount of winter precipitation input, and demonstrates the extremely strong dependence on soil-water status for this water limited mountain island ecosystem.

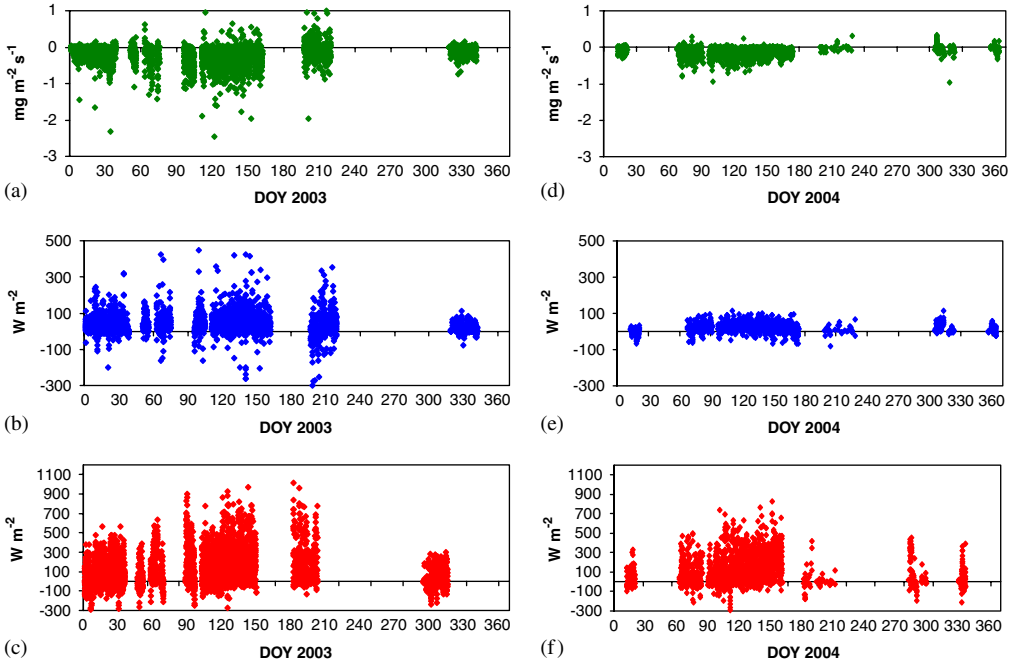

Fig. 4. Daytime fluxes observed at the Mt. Bigelow ec tower for the year 2003; (a) CO_2, (b) Latent heat (evapotranspiration) LE, (c) Sensible heat, and 2004; (d) CO_2, (e) Latent heat (evapotranspiration) LE, (f) Sensible heat, H.

The high precipitation amount for the winter of 2003 is reflected in the large carbon uptake by the trees. Fig. 4 shows that the trees were actively assimilating carbon dioxide throughout the winter season; particularly during February and March when there was persistent snow cover on the ground; at levels greater than any observed for 2004, a year with extremely low winter precipitation. Although there are large data gaps during the fall seasons, observations during the monsoon season, and for periods immediately afterwards indicated that the trees rapidly responded to the influx of monsoon precipitation as indicated by rates of CO_2 uptake greater than immediately before the onset on the summer monsoon.

In this semi-arid environment where water is the significant limiting factor, there is a predominant, direct and immediate correspondence between soil moisture, precipitation (particularly winter) and the rate of photosynthetic activity of the vegetation. The

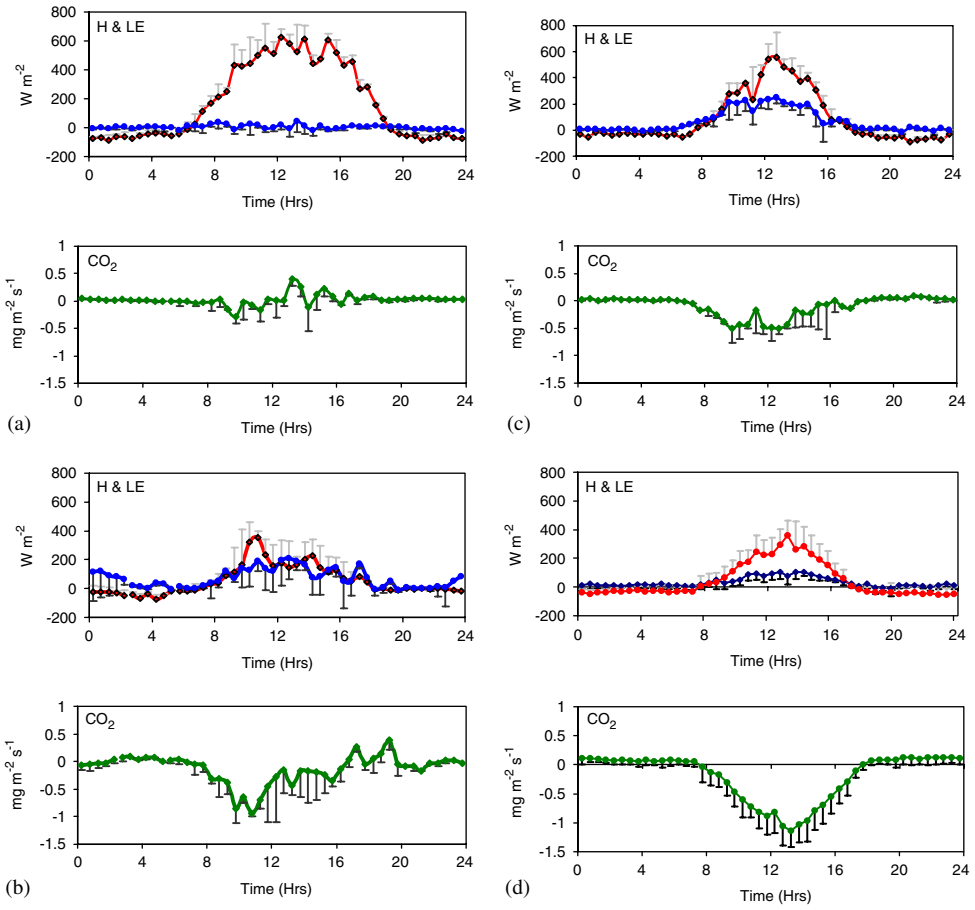

Fig. 5. Surface fluxes observed at the Mt. Bigelow ec tower, averaged over multiple consecutive days, during 2002–2003 pre-monsoon, monsoon, post-monsoon and winter periods. Sensible heat, H (black squares) and latent heat, LE (open circles). (a) 2002 pre-monsoon (DOY 173–175). (b) 2002 monsoon (DOY 250–252). (c) 2002 post-monsoon (DOY 266–268). (d) 2003 winter season (DOY 20–31).

dynamics of the seasonal cycles for this ecosystem can be more fully illustrated by looking at specific time periods as defined by water availability. A series of graphs in Fig. 5 show the corresponding water and CO_2 fluxes for pre-monsoon, monsoon, post-monsoon and winter periods from 2002–2003 (2003–2004 Fig. A4). The fluxes are averaged values for consecutive 3–18 day periods (depending on data availability). The period of greatest moisture stress was during pre-monsoon. The productivity of the trees during this time depended on the amount of winter precipitation. During the pre-monsoon period of 2002, conditions were extremely dry as a result of the extremely low winter precipitation season. Soil moisture peaked at the end of February (42%) and progressively declined to 10% by mid-July of that year (Fig. 3). The trees during this period basically turned off (Fig. 5a) but quickly responded to the strong 2002 monsoon season (Fig. 5b) and the resulting high soil moisture during the post-monsoon period (Fig. 5c). The very strong winter snow season of 2003 is reflected in the very high productivity of the trees during the winter and early spring of that year (Fig. 5d), which is among the highest rates of CO_2 uptake recorded over the 3-year period. The first 3 weeks of March 2003 had persistent below canopy snow cover with correspondingly high soil moisture, and an average air temperature of 1 °C. The soil temperatures were however at or above freezing, providing moisture availability conditions the trees could utilize. The effect of the strong winter snow season is reflected in the following pre-monsoon period of 2003, where the trees remained turned on (Fig. A4a), and the period of low soil moisture was considerably shorter. Surface fluxes for the winter and pre-monsoon seasons of 2004 (Fig. A4a and d) indicate that the productivity levels for the 2004 winter sampled period was much lower than the previous year.

An index of the water use efficiency (WUE) for the forest ecosystem (aggregate soil and vegetation), given as the ratio of CO_2 flux to evaporative flux (F_c/F_w), was calculated for the pre-monsoon, monsoon, post-monsoon and winter sample periods discussed above (Fig. A5). Although the winter period of 2004 had a lower net CO_2 uptake than that of 2003, it had a much higher WUE. This may be a result of higher average air, surface and soil (64 cm depth) temperatures during the sampled period in January of 2003 (6, 2, 4 °C respectively) compared to air, surface and soil temperatures of 2, 1.5 and 2 °C, respectively, during the sampled period in January 2004, resulting in higher soil evaporation. Given an adequate winter season moisture supply (see Fig. 2), the Sky Island forest ecosystem not only has higher rates of CO_2 assimilation but also higher WUE during the winter and spring seasons.

5. Discussion

Most coniferous forests grow at northern latitudes and/or at high altitude in the mid-latitudes. The seasonal behavior of coniferous trees is significantly influenced by temperature changes through the year, either by directly moderating their metabolic rate, or indirectly, by determining the trees access to moisture, such as restricting it in frozen soil or releasing it through snow melt. Consequently, many coniferous forests are largely dormant in winter and have a (sometimes short) summer growing season. The results (shown in Figs. 7 and 8) reveal two interesting features that are noteworthy because they show that the seasonal behavior of mountain island forest growing in the warm semi-arid environment of southern Arizona is substantially different.

During the summer pre-monsoon season (in June 2002) when essentially all the winter precipitation had been evaporated and the soil was extremely dry, the trees essentially

closed down. Daytime CO_2 uptake was very low, evapotranspiration (LE) remained close to zero all day, and the Bowen ratio (H/LE) extremely large because sensible heat flux was the dominant outgoing energy flux. This behavior suggests that trees' ability to access any moisture present in bedrock fractures is not large. Because a late spring/early summer period without any rain is a very common climatic feature in Southern Arizona, the mountain island ecosystem clearly must have evolved the capability to survive it. Fig. 6 shows leaf area index (LAI) and the fraction of photosynthetically active radiation (fpar) absorbed by the vegetation (superimposed on precipitation for the years 2002 and 2003. The LAI reflects the multiyear drought conditions across the region. The significant reduction of fpar during the pre-monsoon period and the immediate rebound at the onset of the monsoon season (indicated by the arrows) is indicative of the reduced (or curtailment of) photosynthetic activity by the trees during this period. The rapid recovery of the forest ecosystem at the onset of the monsoon season (Fig. 6.) confirms the tight coupling between the trees and the available soil moisture.

The wintertime result is the second important and distinctive feature of the seasonal cycle of mountain island forest in this semi-arid environment. During the winter the soil in the rooting zone does not freeze below 4 cm, moisture is available from winter precipitation (rain or snow) and there is adequate radiation for photosynthesis. Vapor

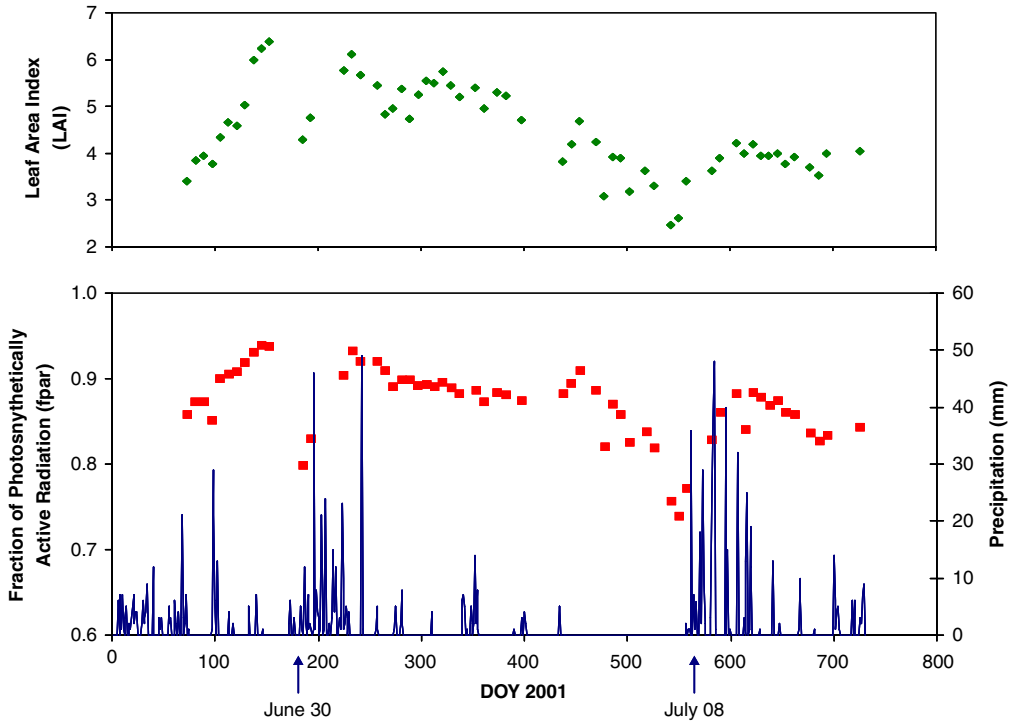

Fig. 6. Biophysical parameters remotely sensed by MODIS on Terra during 2001–2002 for selected forested pixels on Mt. Bigelow. (a) Leaf Area Index (LAI). (b) Fraction of Photosynthetically Active Radiation (FPAR) absorbed by the forest, superimposed on precipitation (mm).

pressure deficit remains reasonably low in these cooler winter months, thus reducing transpiration. As a result of these combined conditions, winter seems to be a favorable time for the forest to sequester carbon. The soil moisture is eventually depleted, however, and the trees once experience heavy soil moisture stress until the monsoon rains return in summer. The adaptation of the semi-arid forest ecosystem to the extremes in the annual cycle of water availability by remaining turned on during the winter with a net CO_2 uptake, is consistent with results from arid-land forest (Grünzweig et al., 2003) where productivity peaks in March and drops to zero at the end of May. The results shown in Figs. 7 and 8 combined with the water use efficiency suggest that any shifts in precipitation from monsoon to winter season would be most beneficial to the south western Sky Island forest ecosystem.

6. Concluding comments

It is well recognized that ecosystems respond to environmental stress (e.g. Law et al., 2002) and, given the complex and somewhat atypical seasonal behavior of semi-arid subalpine mountain island forests described above, extrapolating assumed stress relationships from other western US or temperate coniferous forest as surrogates for mountain island forest is likely fraught with risk. Hopefully the ongoing collection of surface–atmosphere exchange observations at the Mt. Bigelow site will in due course allow better understanding of the physiological behavior of this interesting and unique forest ecosystem, populating the southwestern United States and northern Mexico.

Mountain island forests are important not only because of the control they exert on the regional water budget because they cover land areas which are the primary source of sustainable water resources in this semi-arid region, but also because they likely have a major influence on the regional carbon budget. The seasonal behavior of mountain island forest already apparent in the data reported here from the Mt. Bigelow site is important for any modeling activities in this region. Water stress, rather than temperature, is the primary control on the forest's behavior. The trees will remain significantly active providing they have access to moisture, regardless of the season. It is therefore likely that mountain island forest is a significant and hitherto unrecognized wintertime sink of carbon within the terrestrial carbon balance for this semi-arid region and recognition and representation of this feature in the regional carbon balance merits attention.

Acknowledgments

Primary funding for the research presented in this paper was provided from the National Science Foundation's Science and Technology Center (STC) program through the Center for Sustainability of semi-Arid Hydrology and Riparian Areas (SAHRA) under Agreement EAR-9876800. Additional funding for Eleanor Burke came from NASA contract NAG5-8214. The authors would like to thank the ASRC Jungle Research Group for providing the data acquisition software, John Moncrieff and his research team for the use of EdiRe, members of the NOAA ATDD Laboratory for instrument support, and the many people who assisted in constructing the tower and bringing it into operation.

Appendix

See the Appendix figures (Figs. A1–A5).

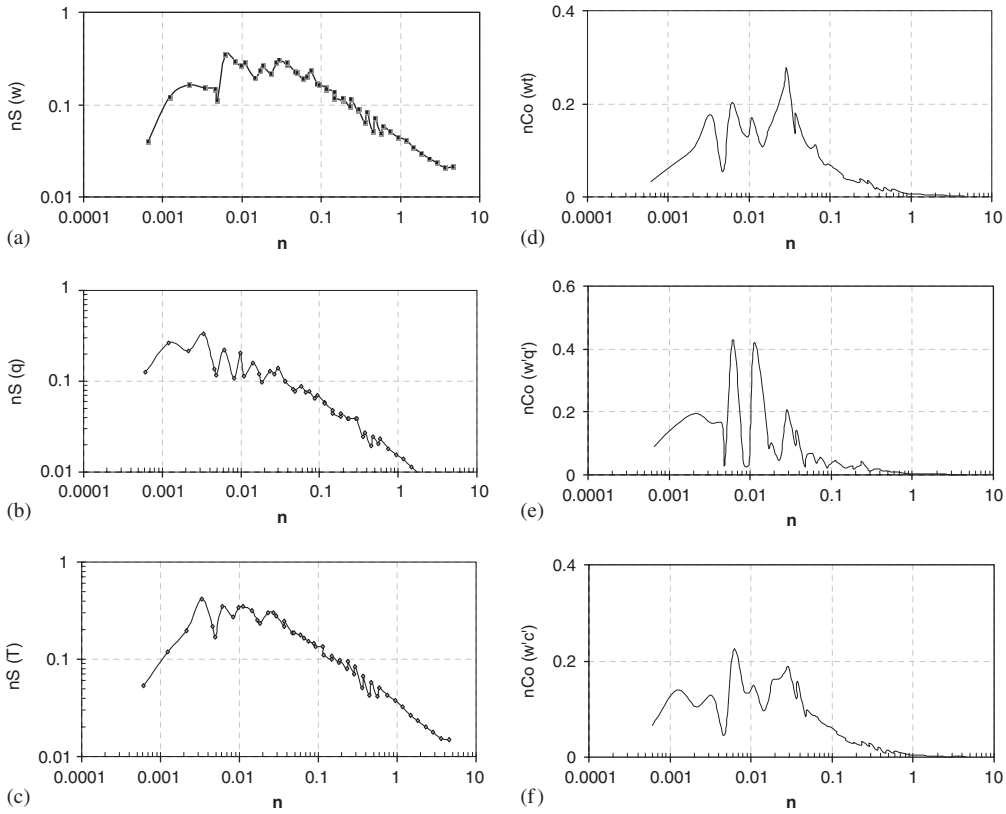

Fig. A1. Spectral analysis of Mt. Bigelow eddy covariance data for June 23, 2002 over ten 30 min segments (08–1300 h). (a) Power spectrum of vertical wind, (b) power spectrum of sonic temperature, (c) power spectrum of water vapor, (d) co-spectrum of the vertical wind and sonic temperature ($w'T'$), (e) co-spectrum of vertical wind and water vapor ($w'q'$) and (f) co-spectrum of vertical wind and CO_2 ($w'c'$).

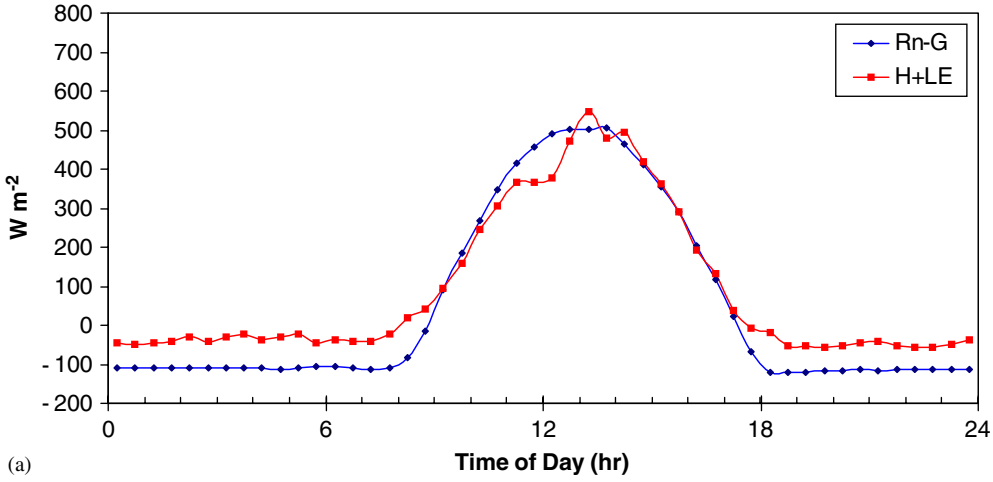

(a)

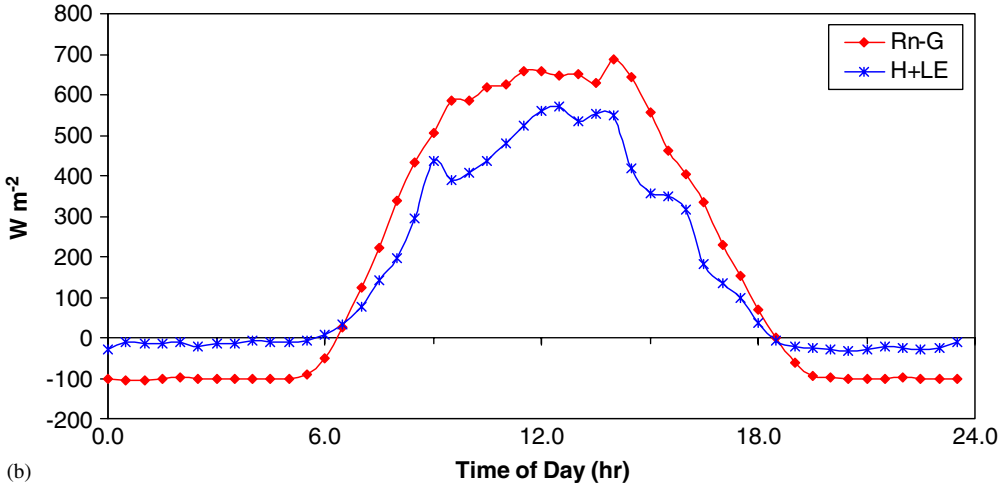

(b)

Fig. A2. Energy Budget, in terms of net radiation-ground heat flux (Rn-G) and the turbulent fluxes of sensible (H) and latent (LE) heat, for (a) January 23–31 2003 (DOY 23–31). (b) May 22–31 2003 (DOY 142–151) observed at the Mt. Bigelow tower.

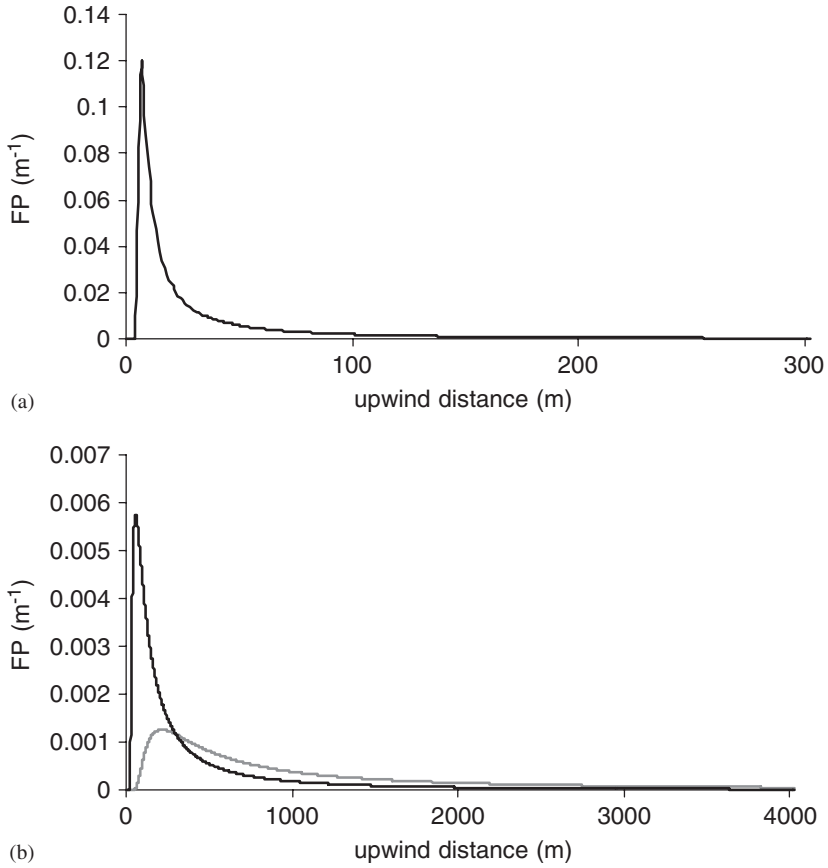

Fig. A3. One-dimensional integrated flux footprint (FP) curves for (a) unstable (largest sensible heat flux), (b) stable (grey lines, smallest sensible heat flux) and near neutral (black lines, largest negative heat flux) conditions for the period of June 2002–January 2003 at the Mt. Bigelow ec tower.

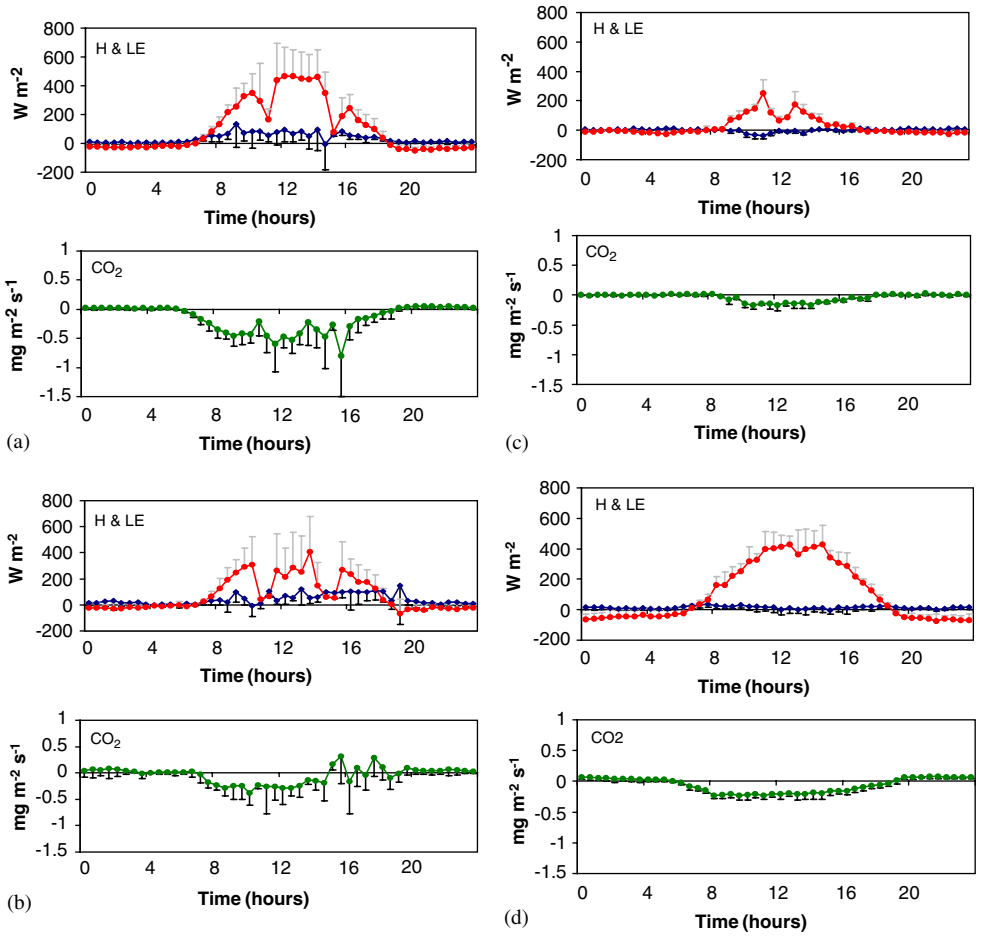

Fig. A4. Surface fluxes observed at the Mt. Bigelow ec tower, averaged over multiple consecutive days, during 2003–2004 pre-monsoon, monsoon, and winter periods. Sensible heat, H (black squares) and latent heat, LE (open circles). (a) 2003 pre-monsoon (DOY 141–154). (b) 2003 monsoon (DOY 208–218). (c) 2004 winter season (DOY 16–21). (d) 2004 pre-monsoon season (DOY 156–173).

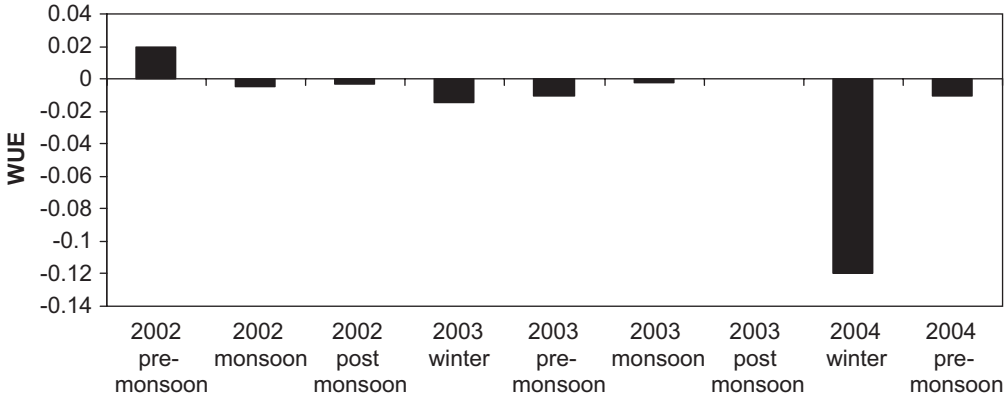

Fig. A5. Water use efficiency (WUE)) of the Mt. Bigelow Forest ecosystem during 2002 pre-monsoon (DOY 173–175), 2002 monsoon (DOY 250–252), 2002 post-monsoon (DOY 266–268), 2003 winter season (DOY 20–31), 2003 pre-monsoon (DOY 141–154), 2003 monsoon (DOY 208–218), 2004 winter season (DOY 16–21) and 2004 pre-monsoon season (DOY 156–173). A positive value indicates net respiration and negative values represent net photosynthesis.

References

Al-Jiboori, M.H., Yumao, Xu., Yongfu, Q., 2000. Turbulence characteristics over complex terrain in West China. Boundary Layer Meteorology 101, 109–126.

Arya, S.P., 1988. In: Dmowska, R., Holton, J. (Eds.), Introduction to Micrometeorology, International Geophysics Series, vol. 42. Academic Press Inc., San Diego pp. 148.

Aubinet, M., Grelle, A., Ibrom, A., Rannik, U., Moncrieff, J., Foken, T., Kowalski, A.S., Martin, P.H., Berbigier, P., Bernhofer, C., Clement, R., Elbers, J., Granier, A., Grunwald, T., Morgenstern, K., Pilegaard, K., Rebmann, C., Snijders, W., Valentini, R., Vesala, T., 2000. Estimates of the annual net carbon and water exchange of forests: The EUROFLUX methodology. Advances in Ecological Research 30, 113–175.

Aubinet, M., Heinesch, B., Yernaux, M., 2003. Horizontal and vertical CO_2 advection in a sloping forest. Boundary Layer Meteorology 108 (3), 397–417.

Baldocchi, D.D., Vogel, C., 1996. Energy and CO_2, flux densities above and below a temperate broadleaf forest and a boreal pine forest. Tree Physiology 16, 5–16.

Baldocchi, D.D., Vogel, C.A., Hall, B., 1997. Seasonal variation of energy and water vapour exchange rates above and below a boreal jack pine canopy. Journal of Geophysical. Research 102 (D24), 28,939–28,951.

Baldocchi, D., Finnigan, J., Wilson, K., Paw, U.K.T., Falge, E., 2000. On measuring net ecosystem carbon exchange over tall vegetation on complex terrain. Boundary Layer Meteorology 96 (1-2), 257–291.

Brown-Mitic, C.M., MacPherson, I.J., Schuepp, P.H., Nagarajan, B., Yau, P.M.K., Bales, R., 2001. Aircraft observations of surface–atmosphere exchange during and after snow melt for different arctic environments: MAGS 1999. Hydrological Processes 15, 3,585–3,602.

Carey, S.K., Woo, M.-K., 2001. Spatial variability of hillslope water balance, wolf creek basin, subarctic yukon. Hydrological Processes 15, 31113–33132.

Carrara, A., Kowalski, A.S., Neirynck, J., Janssens, I.A., Yuste, J.C., Ceulemans, R., 2003. Net ecosystem CO_2 exchange of mixed forest in Belgium over 5 years. Agricultural and Forest Meteorology 119 (3–4), 209–227.

Eugster, W., Rouse, W.R., Pielke, R.A., McFadden, J.P., Baldocchi, D.D., Kittel, T.G.F., Chapin, F.S., Liston, G.E., Vidale, P.L., Vaganov, E., Chambers, S., 2000. Land–atmosphere energy exchange in Arctic tundra and boreal forest: available data and feedbacks to Climate. Global Change Biology 6, 84–115.

Farah, H.O., Bastiaanssen, W.G.M., 2001. Impact of spatial variations of land surface parameters on regional evaporation: a case study with remote sensing data. Hydrological Processes 15, 1585–1607.

Finnigan, J., 1999. A comment on the paper by Lee (1998): "On micrometeorological observations of surface-air exchange over tall vegetation". Agricultural and Forest Meteorology 97 (1), 55–64.

Geissbuhler, P., Siegwolf, R., 2000. Eddy covariance measurements on mountain slopes: The advantage of surface-normal sensor orientation over a vertical set-up. Boundary Layer Meteorology 96, 371–392.

Gilmanov, T.G., Verma, S.B., Sims, P.L., Meyers, T.P., Bradford, J.A., Burba, G.G., Suyker, A.E., 2003. Gross primary production and light response parameters of four Southern Plains ecosystems estimated using long-term CO_2-flux tower measurements. Global Biogeochemical Cycles 17 (2) Art. 1071.

Gochis, D.J., Brito-Castillo, L., Shuttleworth, W.J., 2006. Hydroclimatology of the North American Monsoon region in northwest Mexico. Journal of Hydrology 316, 53–70.

Grünzweig, J.M., Lin, T., Rotenberg, E., Schwartz, A., Yakir, D., 2003. Carbon sequestration in arid-land forest. Global Change Biology 9 (5), 791–799.

Horst, T.W., 1999. The footprint for estimation of atmosphere-surface exchange fluxes by profile techniques. Boundary Layer Meteorology 90 (2), 171–188.

Horst, T.W., Weil, J.C., 1992. Footprint estimation for scalar flux measurements in the atmospheric surface layer. Boundary Layer Meteorology 59, 279–296.

Horst, T.W., Weil, J.C., 1994. How far is far enough?: the fetch requirements of micrometeorological measurements of surface fluxes. Journal of Atmospheric and Oceanic Technology 11, 1,018–1,025.

Kaharabata, S.K., Schuepp, P.H., Ogunjemiyo, S.O., Shen, S., Leclerc, M.Y., Desjardins, R.L., MacPherson, J.I., 1999. Footprint considerations in BOREAS. Journal of Geophysical Research 104 (D22), 29,1 13–29,124.

Kaimal, J.C., Finnigan, J.J., 1994. Boundary Layer Flows. Oxford University Press, Oxford, 289 pp.

Koster, R.D., Suarez, M.J., 1992. Modelling the land surface boundary in climate models as a composite of independent vegetation stands. Journal of Geophysical Research 97 (D3), 2697–2715.

Law, B.E., Falge, E., Gu, L., Baldocchi, D.D., Bakwin, P., Berbigier, P., Davis, K., Dolman, A.J., Falk, M., Fuentes, J.D., Goldstein, A., Granier, A., Grelle, A., Hollinger, D., Janssens, I.A., Jarvis, P., Jensen, N.O., Katul, G., Mahli, Y., Matteucci, G., Meyers, T., Monson, R., Munger, W., Oechel, W., Olson, R., Pilegaard, K., Paw, K.T., Thorgeirsson, H., Valentini, R., Verma, S., Vesala, T., Wilson, K., Wofsy, S., 2002. Environmental controls over carbon dioxide and water vapor exchange of terrestrial vegetation. Agricultural and Forest Meteorology 113 (1–4), 97–120.

Lee, X.H., 1998. On micrometeorological observations of surface-air exchange over tall vegetation. Agricultural and Forest Meteorology 91 (1–2), 39–49.

Lee, X., Hu, Xinzhang, 2002. Forest-Air flux of carbon, water and energy over non-flat terrain. Boundary Layer Meteorology 103 (2), 277–301.

Leuning, R., Judd, M.J., 1996. The relative merits of open- and closed-path analysers for measurement of eddy fluxes. Global Change Biology 2 (3), 241–253.

Mackay, M.D., Stewart, R.E., Bergeron, G., 1998. Downscaling the hydrological cycle in the Mackenzie Basin with the Canadian Regional Climate Model. Atmosphere-ocean 36, 179–211.

Mahrt, L., Lee, X., Black, A., Newman, H., Staebler, R.M., 2000. Nocturnal mixing in a forest subcanopy. Agricultural and Forest Meteorology 101 (1), 67–78.

Massman, W.J., 2000. A simple method for estimating frequency response corrections for eddy covariance systems. Agricultural and Forest Meteorology 104 (3), 185–198.

Mitic, C.M., Schuepp, P.H., Desjardins, R.L., MacPherson, J.I., 1995. Spatial distribution and co-occurrence of surface-atmosphere energy and gas exchange processes over the CODE grid site. Atmospheric Environment 29, 3,169–3,180.

Monson, R.K., Turnipseed, A.A., Sparks, J.P., Harley, P.C., Scott-Denton, L.E., Sparks, K., Huxman, T.E., 2002. Carbon sequestration in a high-elevation, subalpine forest. Global Change Biology 8 (5), 459–478.

Nakai, Y., Sakamoto, T., Terajima, T., Kitamura, K., Skirai, T., 1999. Energy balance above a boreal coniferous forest: a difference in turbulent fluxes between snow-covered and snow-free canopies. Hydrological Processes 13 (4), 515–529.

National Weather Service Forecast Office, Tucson, Arizona, 〈http://newweb.wrh.noaa.gov/twc/climate/seazDM.php〉.

Neumann, N., Marsh, P., 1998. Local advection in the snowmelt landscape of arctic tundra. Hydrological Processes 12, 1,547–1,560.

Ogunjemiyo, S.O., Schuepp, P.H., MacPherson, J.I., Desjardins, R.L., 1997. Analysis of flux maps vs surface characteristics from Twin Otter grid flights in BOREAS 1994. Journal of Geophysical Research 102 (D24), 29,135–29,145.

Pattey, E., Desjardins, R.L., St-Amour, G., 1997. Mass and energy exchanges over a black spruce forest during key periods of BOREAS 1994. Journal of Geophysical Research 102 (D24), 28,967–28,975.

Rouse, W.R., 2000. The energy and water balance of high-latitude wetlands: controls and extrapolation. Global Change Biology 6 (1), 59–68.

Scott, R.L., Shuttleworth, W.J., Goodrich, C., Maddock III, T., 2000. The water use of two dominant vegetation communities in a semiarid riparian ecosystem. Agricultural and Forest Meteorology 105 (1–3), 241–256.

Shuttleworth, W.J., 1991. Insights from large-scale observational studies of land/atmosphere interactions. Surveys in Geophysics 12, 1–3.

Turnipseed, A.A., Blanken, P.D., Anderson, D.E., Monson, R.K., 2002. Energy budget above a high elevation subalpine forest in complex topography. Agricultural and Forest Meteorology 110 (3), 177–201.

Webb, E.K., Pearman, G.I., Leuning, R., 1980. Correction of flux measurements for density effects due to heat and water-vapor transfer. Quarterly Journal of the Royal Meteorological Society 106 (447), 85–100.

Wilson, K., Goldstein, A., Falge, E., Aubinet, M., Baldocchi, D., Berbigier, P., Bernhofer, C., Ceulemans, R., Dolman, H., Field, C., Grelle, A., Ibrom, A., Law, B.E., Kowalski, A., Meyers, T., Moncrieff, J., Monson, R., Oechel, W., Tenhunen, J., Valentini, R., Verma, S., 2002. Energy balance closure at FLUXNET sites. Agricultural and Forest Meteorology 113 (1–4), 223–243.